Simulations of micro-bending of thin foils using a scale dependent crystal plasticity model*

Mitsutoshi Kuroda[1], **Viggo Tvergaard**[2], **Tetsuya Ohashi**[3]

[1] Department of Mechanical Systems Engineering, Yamagata University, Jonan 4-3-16, Yonezawa, Yamagata 992-8510, Japan

[2] Department of Mechanical Engineering, Solid Mechanics, Technical University of Denmark, DK-2800, Kgs. Lyngby, Denmark

[3] Mechanical Systems Department, Kitami Institute of Technology, Koencho 165, Kitami, Hokkaido 090-8507, Japan

Abstract

In this paper, we perform crystal plasticity analyses of micro-bending of thin f.c.c. metal foils having thicknesses ranging from 10 to 50 micrometers. The scale dependent crystal plasticity model used here is a viscoplastic finite strain version of the model proposed by Ohashi (International Journal of Plasticity 21 (2005) 2071-2088), in which the mean free path of moving dislocations is determined by a function of the densities of statistically stored dislocations and geometrically necessary dislocations, while the slip resistance for each slip system is determined only by the density of statistically stored dislocations through a Bailey-Hirsch type relation. The computational results are compared with experimental results for Ni foils, reported in Stölken and Evans (Acta Materialia 46 (1998) 5109-5115). Validity of the current model and a direction of future development of the "physically-based" scale dependent crystal plasticity models are discussed.

1. Introduction

In a non-homogeneous plastic deformation, dislocations are classified into the statistically stored dislocations (SSD) and geometrically necessary dislocations (GND). The SSDs develop in homogeneous deformation and are said to be ‘redundant’ to establish a given plastically deformed configuration. By contrast, the GNDs are ‘non-redundant’ to accommodate a non-homogeneous deformation, and are directly related to the plastic strain gradients.

From a physical point of view, the GNDs must play a key role in explanation of size effects occurring in the non-homogeneous plastic deformation of small specimens. To represent a size dependence of flow stress behavior, the critical resolved shear stress (slip resistance) τ_c on a slip system is often assumed to be given by the following equation (Fleck

* Author’s manuscript for *Modelling Simul. Mater. Sci. Eng.* Vol. **15** (2007) S13–S22.

et al., 1994; Han et al., 2005), which is a modified version of the classical Taylor relation,

$$\tau_c = c\mu b\sqrt{\rho_S + \rho_G}\ , \tag{1}$$

where c is an empirical coefficient, μ is the elastic shear modulus, b is the magnitude of Burgers vector, ρ_S is the SSD density, and ρ_G is the GND density on the slip system. Eq. (1) makes it possible to model a size effect in the presence of a plastic strain gradient. Some researchers, however, have questioned this idea. Mughrabi (2004) argued that the edge GND density is not expected to appear in the flow stress law in single slip and the GNDs on the same slip system can only act as relatively weak obstacles, unlike forest dislocations that must be cut by the glide dislocations. Weertman (2002) also suggested that only the GNDs which primarily act as forest dislocations contribute the magnitude of the flow stress.

In a bending deformation of thin foil, a large first order plastic strain gradient (i.e. GNDs) is produced through the whole thickness. Thus, the bending problem of thin foil is expected to be suitable for investigating the strain gradient dependent mechanical behavior of metals at the micron scale.

In this paper, we employ a scale dependent crystal plasticity model recently proposed by Ohashi (2004; 2005), in which the slip resistance for each slip system is determined only by the SSD densities (unlike Eq. (1)) through a Taylor type relation, while the mean free path of moving dislocations is determined by a function of both the SSD and GND densities. Using this model, we perform finite element analyses of micro-bending of thin f.c.c. metal foils having thicknesses ranging from 10 to 50 micrometers. The computational results are compared with experimental results for Ni foils, reported in Stölken and Evans (1998). Validity of the current model and a direction of future development of the "physically-based" scale dependent crystal plasticity models are critically discussed

2. Constitutive model

In a single crystal, the velocity gradient $\mathbf{L}$ is decomposed into nonplastic and plastic parts:

$$\mathbf{L} = \mathbf{L}^* + \mathbf{L}^p\ . \tag{2}$$

The plastic contribution $\mathbf{L}^p$ is assumed to arise from slip on a finite number of slip systems:

$$\mathbf{L}^p = \mathbf{D}^p + \mathbf{W}^p = \sum_\alpha \dot\gamma^{(\alpha)}\mathbf{p}^{(\alpha)} + \sum_\alpha \dot\gamma^{(\alpha)}\mathbf{w}^{(\alpha)}\ , \tag{3}$$

$$\mathbf{p}^{(\alpha)} = \frac{1}{2}(\mathbf{s}^{(\alpha)} \otimes \mathbf{m}^{(\alpha)} + \mathbf{m}^{(\alpha)} \otimes \mathbf{s}^{(\alpha)})\ , \tag{4}$$

$$\mathbf{w}^{(\alpha)} = \frac{1}{2}(\mathbf{s}^{(\alpha)} \otimes \mathbf{m}^{(\alpha)} - \mathbf{m}^{(\alpha)} \otimes \mathbf{s}^{(\alpha)})\ , \tag{5}$$

where $\mathbf{D}^p$ is the plastic rate of deformation (symmetric part of $\mathbf{L}^p$), $\mathbf{W}^p$ is the plastic spin (anti-symmetric part of $\mathbf{L}^p$), $\dot\gamma^{(\alpha)}$ is the slip rate, $\mathbf{s}^{(\alpha)}$ is the slip direction and $\mathbf{m}^{(\alpha)}$ is the slip plane normal for the α th slip system. In the present applications, the $\{111\}\ \langle 1\bar{1}0\rangle$ twelve slip systems for f.c.c. metals are adopted.

Allowing for finite lattice rotations, the nonplastic contribution $\mathbf{L}^*$ is related to the stress rate as follows:

$$\overset{\nabla}{\boldsymbol{\sigma}}{}^* = \dot{\boldsymbol{\sigma}} - \mathbf{W}^* \cdot \boldsymbol{\sigma} + \boldsymbol{\sigma} \cdot \mathbf{W}^* = \mathbf{C} : \mathbf{D}^* = \mathbf{C} : \mathbf{D} - \sum_\alpha \dot\gamma^{(\alpha)}\mathbf{C} : \mathbf{p}^{(\alpha)}\ , \tag{6}$$

$$\mathbf{D}^* = \frac{1}{2}(\mathbf{L}^* + \mathbf{L}^{*\mathrm{T}}), \tag{7}$$

$$\mathbf{W}^* = \frac{1}{2}(\mathbf{L}^* - \mathbf{L}^{*\mathrm{T}}), \tag{8}$$

where $\boldsymbol{\sigma}$ is the Cauchy stress, $\overset{\nabla}{\boldsymbol{\sigma}}{}^*$ is the lattice Jaumann rate with respect to $\mathbf{W}^*$, $\mathbf{D}$ is the rate of deformation tensor (symmetric part of $\mathbf{L}$), the superscript T denotes 'transpose', and $\mathbf{C}$ is a fourth-order elastic moduli tensor. The lattice vectors $\mathbf{s}^{(\alpha)}$ and $\mathbf{m}^{(\alpha)}$ are rotated by

$$\dot{\mathbf{s}}^{(\alpha)} = \mathbf{W}^* \cdot \mathbf{s}^{(\alpha)}, \qquad \dot{\mathbf{m}}^{(\alpha)} = \mathbf{W}^* \cdot \mathbf{m}^{(\alpha)}. \tag{9}$$

The constitutive description for a single crystal is completed by specifying the relation for $\dot{\gamma}^{(\alpha)}$. As in Peirce et al. (1983), the slip rate $\dot{\gamma}^{(\alpha)}$ is assumed to be given by a power law dependence on the resolved shear stress $\tau^{(\alpha)}$ on slip system α,

$$\dot{\gamma}^{(\alpha)} = \dot{\gamma}_0 \,\mathrm{sgn}(\tau^{(\alpha)}) \left| \frac{\tau^{(\alpha)}}{g^{(\alpha)}} \right|^{1/m}, \qquad \tau^{(\alpha)} = \mathbf{p}^{(\alpha)} : \boldsymbol{\sigma} \tag{10}$$

where $\dot{\gamma}_0$ is a reference slip rate, m is the strain rate sensitivity exponent, and $g^{(\alpha)}$ is the slip system hardness. The $g^{(\alpha)}$ is defined as a function of the density of accumulated SSD:

$$g^{(\alpha)} = g_0^{(\alpha)} + \sum_{\beta} \Omega^{(\alpha\beta)} c\mu b \sqrt{\rho_{\mathrm{S}}^{(\beta)}}\,. \tag{11}$$

Here, the first term $g_0^{(\alpha)}$ gives the lattice friction for movement of dislocations, which is, in general, very small for f.c.c. crystals. The second term represents the effect of accumulated dislocations on moving dislocations: $\rho_{\mathrm{S}}^{(\beta)}$ denotes the SSD density on the slip system β, c is an empirical coefficient (the order of 0.1), μ is the elastic shear modulus, b is the magnitude of Burgers vector, and $\Omega^{(\alpha\beta)}$ is an interaction matrix for dislocations on slip systems α and β. The GND densities do not directly enter the slip hardening law in Eq. (11) (Ohashi, 2004; 2005), as mentioned in the Introduction.

The evolution of the SSD density is modeled as

$$\dot{\rho}_{\mathrm{S}}^{(\alpha)} = \frac{1}{bL^{(\alpha)}} \left| \dot{\gamma}^{(\alpha)} \right|, \tag{12}$$

where $L^{(\alpha)}$ is the mean free path of dislocations on the slip system α. The physical interpretation and detailed derivation of Eq. (12) have been explained in Ohashi (1994). A similar evolution law with an "annihilation term" (Essmann and Mughrabi, 1979) is often used (e.g. Evers et al., 2004). In the present application, we will investigate the material behavior at small or moderate strains and at room temperature. It is expected that the additional term will not have a big influence under these conditions. Thus, it is not considered for simplicity. The mean free path of moving dislocations is taken to be given by

$$L^{(\alpha)} = K \cdot l^{(\alpha)}, \qquad l^{(\alpha)} = \frac{1}{\sqrt{\sum_{\beta \neq \alpha} \left(a_1 \rho_{\mathrm{S}}^{(\beta)} + a_2 \left\| \rho_{\mathrm{G}}^{(\beta)} \right\| \right)}}. \tag{13}$$

Here, $l^{(\alpha)}$ represents an effective average distance between forest dislocations, which obstruct movement of dislocations on slip system α. $\left\| \rho_{\mathrm{G}}^{(\beta)} \right\|$ denotes the norm of the GND density on slip system β, defined as

$$\left\|\rho_{\mathrm{G}}^{(\beta)}\right\| = \sqrt{(\rho_{\mathrm{G,edge}}^{(\beta)})^2 + (\rho_{\mathrm{G,screw}}^{(\beta)})^2}\,, \tag{14}$$

with the edge and screw components given by gradients in slip (Ashby, 1970; Fleck et al., 1994):

$$\rho_{\mathrm{G,edge}}^{(\beta)} = -\frac{1}{b}\frac{\partial \gamma^{(\beta)}}{\partial \xi^{(\beta)}}, \qquad \rho_{\mathrm{G,screw}}^{(\beta)} = \frac{1}{b}\frac{\partial \gamma^{(\beta)}}{\partial \zeta^{(\beta)}}, \tag{15}$$

where, $\xi^{(\beta)}$ and $\zeta^{(\beta)}$ are directions parallel and perpendicular to the slip directions on the slip plane. In Eq. $(13)_2$, a_1 and a_2 are parameters that control contributions of SSD and GND densities to $l^{(\alpha)}$. A coefficient K in Eq. $(13)_1$ represents the assumed number of forest dislocations that are cut by a moving dislocation before it ceases to move (usually K is assumed to be in a range of 10 – 100). In the present model, the GND densities that are gradients in slip cut the mean free paths of moving dislocations on other slip systems, and thus a size dependent strain hardening appears.

The crystal plasticity model shown above does not involve any higher-order stress quantities or extra slip boundary conditions, such that equilibrium equations and boundary conditions are identical to those in classical plasticity theories. Only the constitutive equations are improved to account for the effect of the GND densities. This approach is similar to that proposed by Han et al. (2005). But, the present constitutive modeling that involves the effect of the GND densities is different from their proposition based on Eq. (1).

3. Problem formulation and numerical procedure

The problem is concerned with a micro-bending of thin foils under plane strain states (Stölken and Evans, 1998). Annealed Ni foils having thicknesses H = 12.5, 25 and 50 μm were used in their experiments. Grain sizes were about equal to the foil thickness. The foils were plastically bent around a small cylindrical bar by means of loads applied through a profiled die. In the present computational study, such a bending process is simply modeled by pure bending as shown in **figure 1**. A polycrystal model with five square grains is considered. The aspect ratio, L/H, of the region is taken to be 5.

We apply the pure bending deformation to the specimen as follows. Taking the points, about which the vertical edges $X_1 = L$ and $X_1 = 0$ rotate, to be on the middle line $X_2 = H/2$, the boundary conditions on the edges are expressed as (Triantafyllidis et al., 1982; Kuroda and Tvergaard, 2004):

$$u_1 \cos\left(\pm\frac{\theta}{2}\right) - \left(u_2 + X_2 - \frac{H}{2}\right)\sin\left(\pm\frac{\theta}{2}\right) = 0\,, \tag{16}$$

$$q_1 \sin\left(\pm\frac{\theta}{2}\right) + q_2 \cos\left(\pm\frac{\theta}{2}\right) = 0\,, \tag{17}$$

where θ is the bending angle, the plus sign in front of θ is for $X_1 = L_0$ and the minus sign is for $X_1 = 0$, u_i are the displacement components, and q_i are the components of the surface traction per current area of surface. The bending moment is given by

$$M_{\mathrm{b}} = \int_{r_{\mathrm{i}}}^{r_{\mathrm{o}}} q_{\mathrm{n}} r \mathrm{d}r \quad \text{on} \quad X_1 = 0\,, \tag{18}$$

where q_{n} is the surface traction per current area of surface, which is normal to the edge surface, r is a coordinate along the edge $X_1 = 0$, r_{i} and r_{o} are, respectively, the inner and

outer radii of the bent specimen. The rate of bending is given as $\dot{\theta} = \dot{\gamma}_0 L / H$.

Grain orientations are randomly assigned, corresponding to the sample condition in the experimental study[1] (Stölken and Evans, 1998). Each grain is discretized by 20 × 20 plane strain quadrilateral eight node finite elements with reduced integration. A standard updated Langangian finite element scheme (McMeeking and Rice, 1975) is employed.

The spatial gradients in slip are needed to compute the GND densities, $\rho_{\mathrm{G}}^{(\alpha)}$. First, nodal values of slip for each element are evaluated by extrapolations from the integration point values. The nodal values of slip as a field quantity are calculated as the average of the nodal values in all the elements connected to the node. Then, the gradients in slip are computed by use of the derivatives of the finite element shape functions.

4. Results

Values of material parameters used in the present numerical computations are shown in Table 1. For the relation for mean free path (Eq. (13)), we take $a_1 = 0$ and $a_2 = 1$ so that the strongest possible size effect appears. If we used a larger value of a_1, the size dependence would simply diminish compared to the present results shown below. According to Eq. (13), the computed mean free path $L^{(\alpha)}$ may exceed the "grain size" at the initial stage of deformation. This is physically impossible. In this case, we assume that $L^{(\alpha)}$ is restricted to the grain size, which is approximated by the length H in the present application.

The mechanical responses are affected by randomly chosen grain orientations. We performed 6 sets of computations using 6 different series of pseudo-random numbers. **Figure 2** shows computed curves of normalized bending moment verses normalized curvature for three selected sets of grain orientations including those that have predicted the largest and smallest bending moments. In the graph, B denotes the width of the specimen. For each set of computations, a clear size dependence is observed: i.e. the smallest specimen ($H = 12.5\,\mu\mathrm{m}$) exhibits the largest bending moment. In **figure 3**, one of the computational results (i.e. the middle set in figure 2) is compared to the experimental result of Stölken and Evans (1998). As mentioned above, we have assumed that the mean free path is fully determined by the GND densities, and this choice yields the maximum size effect in this model. Nevertheless, the predicted size effect seems to be somewhat smaller than the experimentally observed one. It is noted that the "initial yield stresses" for the three foils with different thicknesses are predicted to be the same because the size effect is only the consequence of the plastic strain gradients. This point will be discussed later.

Figure 4 shows distributions of the GND density, $\left\|\rho_{\mathrm{G}}^{(\alpha)}\right\|$, in the primary slip system in each grain for $H = 12.5\ \mu\mathrm{m}$. In the cases of the other two sizes (i.e. $H = 25$ and $50\ \mu\mathrm{m}$), although illustrations are omitted here, distributions of the GND densities are almost identical to the one shown in **figure 4**, but with reduced magnitudes that are almost inversely proportional to the thickness.

Figure 5 shows distributions of the SSD density, $\rho_{\mathrm{S}}^{(\alpha)}$, in the primary slip system in each grain for $H = 12.5\ \mu\mathrm{m}$. As expected, higher SSD densities are observed near the free surfaces, while no accumulation of the SSD is predicted along the neutral surface of bending. The SSD density distributions for $H = 25$ and $50\ \mu\mathrm{m}$ are very similar to those shown in $H = 12.5\ \mu\mathrm{m}$, but illustrations of these cases are omitted here. But, the SSD densities are also strongly size

[1] As long as we can see from the pole figure shown in Stölken and Evans (1998), the random orientation model is expected to give a good approximation.

dependent, because their evolution is governed by the GND density dependent mean free paths (Eqs. (12) and (13)). For example, the largest value of $\rho_S^{(\alpha)}$ for H = 12.5 μm is 1.08×10^9 mm^{-2}, and for H = 25 and 50 μm they are respectively, 7.72×10^8 and 5.47×10^8 mm^{-2}, which are approximately inversely proportional to $\sqrt{H}$.

5. Discussion

Hardening laws in the spirit of Eq. (1) have been widely adopted since Fleck et al. (1994) (e.g. Han et al. (2005)). As pointed out in the Introduction, however, it has been argued that the edge GND density is not expected to appear in the flow stress law under single slip conditions and the GNDs on the same slip system can only act as relatively weak obstacles, unlike forest dislocations that must be cut by the glide dislocations (Mughrabi, 2004). It has also been suggested by Weertman (2002) that only the GNDs, which play the role of forest dislocations, contribute to the magnitude of the flow stress. The slip hardening model used here (Ohashi, 2004), Eqs. (11)–(14), follows such suggestions. Acharya et al. (2003) also tried to represent an extra hardening effect arising from reduction of the mean free path due to existence of geometric dislocations, introducing an obstacle density defined with Nye's dislocation density tensor. By contrast, in our model, the mean free path is explicitly determined with the SSD and GND densities on each slip system (Eq. (13)).

The present constitutive theory involves neither higher order stress quantities nor extra slip boundary conditions, unlike Gurtin (2002), Arsenlis et al. (2004), Evers et al. (2004), Yefimov et al. (2004; 2005). According to the study by Huang et al. (2004), it is expected that higher order slip boundary conditions affect the material response only within a thin boundary layer (the order of sub micron in size) of the solid and hardly influence the overall mechanical responses of the specimens with the size larger than ten microns as in the present application. A detailed study for a higher order scale dependent crystal plasticity theories with extra slip boundary conditions is carried out in a separate paper (Kuroda and Tvergaard, 2006).

Shrotriya et al. (2003) also carried out an experimental study for a size dependent behavior of nickel foils in micro-bend tests, and observed a degree of the size dependence, which is close to that reported in Stölken and Evans (1998). The present model seems to give a size dependence smaller than that observed in the experimental studies, as seen in **figure 3**.

In the experiments of Stölken and Evans (1998), it was observed that (i) the strain hardening was essentially linear and about the same for all foil thicknesses, and (ii) the initial yield strength *increased* as the foil thickness *increased* for uniaxial tensile tests, opposite to the usual understanding. In their micro-bend tests, however, (i) the strain hardening clearly increased as the foil thickness *decreased*, and (ii) a larger initial yield stress for a smaller foil thickness could be recognized (**figure 3**), although this is not so obvious since the measurements were not continuous. Thus, no unified understanding for size effects in tension and bending could be gained from their experimental results. In the present constitutive model, the size effect only arises from gradients in total *plastic* slip. Therefore, the *initial yield stress* as a limit of elastic response predicted by the present model exhibits no size dependence, as seen in **figure 3**. In a strict sense, only the strain hardening behaviors in the experiments and the computations might have been compared.

Several investigations for the size dependence of initial yielding have been carried out experimentally (Uchic et al., 2004; Dimiduk et al., 2005) and computationally (Benzerga and Shaver, 2006; Ohashi et al., 2006). In these computational approaches, the size dependence of initial yielding is attributed to a scale effect of dislocation sources, i.e. in principle a smaller dislocation source requires a larger applied shear stress to bow out. Anand et al. (2005) and Fredriksson and Gudmundson (2005) suggested that a dissipative gradient effect associated

with the plastic strain *rate* gradient represents the size dependence of initial yielding in a gradient field. Introduction of a size dependence of initial yielding into the constitutive model is worth pursuing. But then, we should carefully investigate the actual source of the size dependence of initial yielding in micro-bend tests.

Acknowledgement

The assistance of the numerical computations by Mr. Takahiro Shikama is gratefully acknowledged.

References

Acharya, A., Bassani, J.L., Beaudoin, A., 2003. Geometrically necessary dislocations, hardening, and a simple gradient theory of crystal plasticity. Scripta Materialia 48, 167-172.

Anand, L., Gurtin, M.E., Lele, S.P., Gething, C., 2005. A one-dimensional theory of strain-gradient plasticity: Formulation, analysis, numerical results. Journal of the Mechanics and Physics of Solids 53, 1789-1826.

Arsenlis, A., Parks, D.M., Becker, R., Bulatov, V.V., 2004. On the evolution of crystallographic dislocation density in non-homogeneously deforming crystals. Journal of the Mechanics and Physics of Solids 52, 1213-1246.

Ashby, M.F., 1970. The deformation of plastically non-homogeneous materials. Philosophical Magazine 21, 399-424.

Benzerga, A.A., Shaver, N.F., 2006. Scale dependence of mechanical properties of single crystals under uniform deformation. Scripta Materialia 54, 1937-1941.

Dimiduk, D.M., Uchic, M.D., Parthasarathy, T.A., 2005. Size-affected single-slip behavior of pure nickel microcrystals. Acta Materialia 53, 4065–4077.

Essmann, U., Mughrabi, H., 1979. Annihilation of dislocations during tensile and cyclic deformation and limits of dislocation densities. Philosophical Magazine A40, 731-756.

Evers, L.P., Brekelmans, W.A.M., Geers, M.G.D., 2004. Non-local crystal plasticity model with intrinsic SSD and GND effects. Journal of the Mechanics and Physics of Solids 52, 2379-2401.

Fleck, N.A., Muller, G.M., Ashby, M.F., Hutchinson, J.W., 1994. Strain gradient plasticity: theory and experiment. Acta Metallurgica et Materialia 42, 475-487.

Fredriksson, P., Gudmundson, P., 2005. Size-dependent yield strength of thin films. International Journal of Plasticity 21, 1834–1854.

Gurtin, M.E., 2002. A gradient theory of single-crystal viscoplasticity that accounts for geometrically necessary dislocations. Journal of the Mechanics and Physics of Solids 50, 5-32.

Han, C.-S., Gao, H., Huang, Y., Nix, W.D., 2005. Mechanism-based strain gradient crystal plasticity–I. Theory. Journal of the Mechanics and Physics of Solids 53, 1188-1203.

Huang, Y., Qu, S., Hwang, K.C., Li, M., Gao, H., 2004. A conventional theory of mechanism-based strain gradient plasticity. International Journal of Plasticity 20, 753-782.

Kuroda, M., Tvergaard, V., 2004. Shear band development in anisotropic bent specimens. European Journal of Mechanics A/Solids 23, 811-821.

Kuroda, M., Tvergaard, V., 2006. Studies of scale dependent crystal viscoplasticity models.

Journal of the Mechanics and Physics of Solids 54, 1789-1810.
McMeeking, R. M., Rice, J. R., 1975. Finite-element formulations for problems of large elastic-plastic deformation. International Journal of Solids and Structures 11, 601-616.
Mughrabi, H., 2004. On the current understanding of strain gradient plasticity. Materials Science and Engineering A387, 209-213.
Ohashi, T., 1994. Numerical modelling of plastic multislip in metal crystals of f.c.c. type. Philosophical Magazine A70, 793-803.
Ohashi, T., 2004. A new model of scale dependent crystal plasticity analysis. In: H. Kitagawa and Y. Shibutani, Eds., Solid mechanics and its applications, vol. 115, Proceedings of IUTAM Symposium on Mesoscopic Dynamics in Fracture Process and Strength of Materials, Osaka, Japan, Kluwer Academic Publishers, Dordrecht, pp. 97–106.
Ohashi, T., 2005. Crystal plasticity analysis of dislocation emission from micro voids. International Journal of Plasticity 21, 2071–2088.
Ohashi, T., Kawamukai, M., Zbib, H.M., 2006. A multiscale approach for modeling scale-dependent yield stress in polycrystalline metals. International Journal of Plasticity (to be published).
Peirce, D., Asaro, R. J., Needleman, A., 1983. Material rate dependence and localized deformation in crystalline solids. Acta Metallurgica 31, 1951-1976.
Shrotriya, P., Allameh, S.M., Lou, J., Buchheit, T., Soboyejo, W.O., 2003. On the measurement of the plasticity length scale parameter in LIGA nickel foils. Mechanics of Materials 35, 233–243.
Stölken, J.S., Evans, A.G., 1998. A microbend test method for measuring the plasticity length scale. Acta Materialia 46, 5109-5115.
Triantafyllidis, N., Needleman, A., Tvergaard, V., 1982. On the development of shear bands in pure bending. International Journal of Solids and Structures 18, 121-138.
Uchic, M.D., Dimiduk, D.M., Florando, J.N., Nix, W.D., 2004. Sample dimensions influence strength and crystal plasticity. Science 305, 986-989.
Weertman, J., 2002. Anomalous work hardening, non-redundant screw dislocations in a circular bar deformed in torsion, and non-redundant edge dislocations in a bent foil. Acta Materialia 50, 673-689.
Yefimov, S., Groma, I., van der Giessen, E., 2004. A comparison of a statistical-mechanics based plasticity model with discrete dislocation plasticity calculations. Journal of the Mechanics and Physics of Solids 52, 279-300.
Yefimov, S., van der Giessen, E., 2005. Multiple slip in a strain-gradient plasticity model motivated by a statistical-mechanics description of dislocations. International Journal of Solids and Structures 42, 3375–3394.

Table and Figure Captions

Table 1. Constitutive parameters.

Figure 1. Problem formulation of pure bending of a thin foil with grain size being about equal to the thickness.

Figure 2. Appearance of size effect on computed curves of bending moment versus bending angle for three sets of randomly chosen grain orientations.

Figure 3. Comparison of computed curves of bending moment versus bending angle to experimental results of Stölken and Evans (1998).

Figure 4. Deformed configurations of the foil ($H = 12.5\ \mu\text{m}$) and contours of GND densities on primary slip system at (a) $\theta H / L = 0.013$, (b) $\theta H / L = 0.123$, and (c) $\theta H / L = 0.178$.

Figure 5. Deformed configurations of the foil ($H = 12.5\ \mu\text{m}$) and contours of SSD densities on primary slip system at (a) $\theta H / L = 0.013$, (b) $\theta H / L = 0.123$, and (c) $\theta H / L = 0.178$.

Table 1. Constitutive parameters.

Parameter	Symbol	Magnitude	Unit
Young's modulus	E	220	GPa
Poisson's ratio	ν	0.3	–
Burgers vector	b	0.249	nm
Initial SSD density	$\rho_{S0}^{(\alpha)}$	10^6	mm^{-2}
Material constant	K	11	–
Numerical coefficient	a_1, a_2	0, 1.0	–
Lattice friction	$g_0^{(\alpha)}$	1.0	MPa
Interaction matrix	$\Omega^{(\alpha\beta)}$	All 1.0	–
Empirical coefficient	c	0.1	–
Reference plastic strain rate	$\dot{\gamma}_0$	1	s^{-1}
Rate sensitivity exponent	m	0.002	–

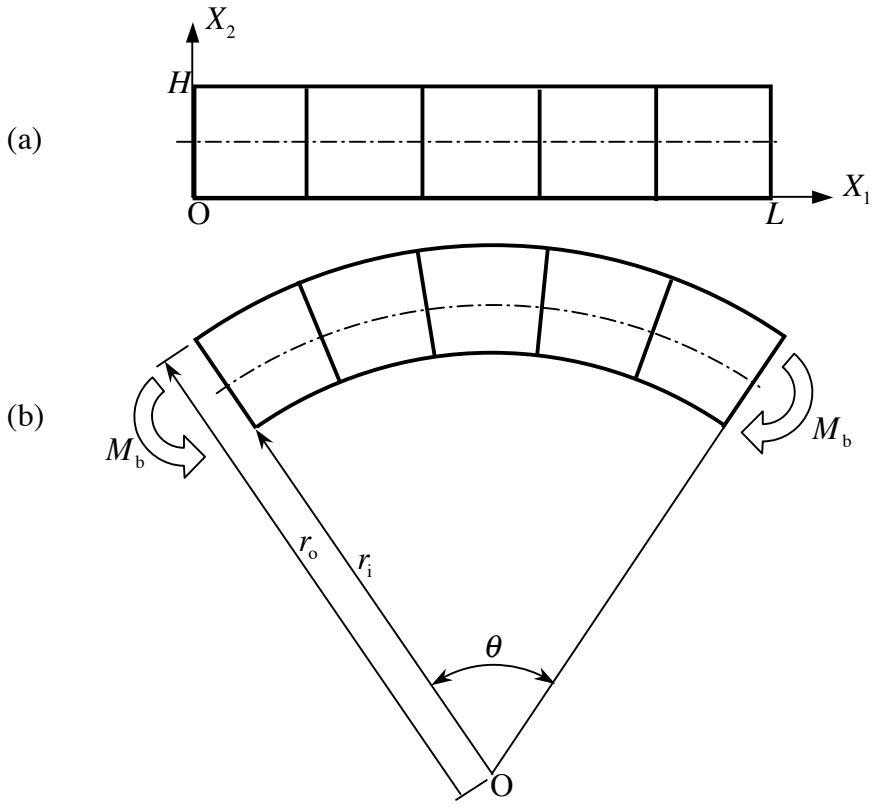

Figure 1. Problem formulation of pure bending of a thin foil with grain size being about equal to the thickness.

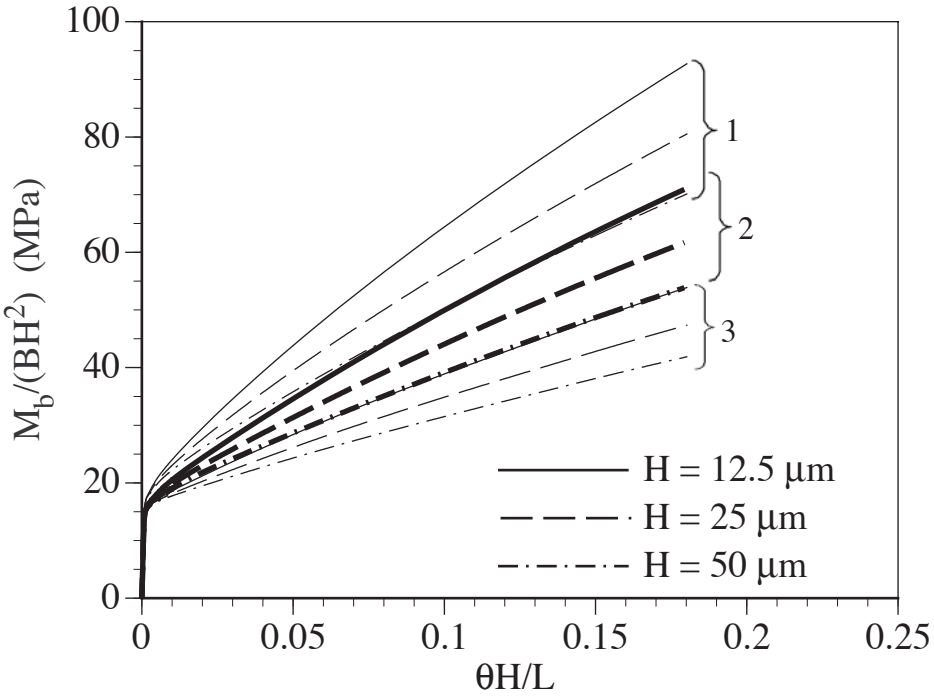

Figure 2. Appearance of size effect on computed curves of bending moment versus bending angle for three sets of randomly chosen grain orientations.

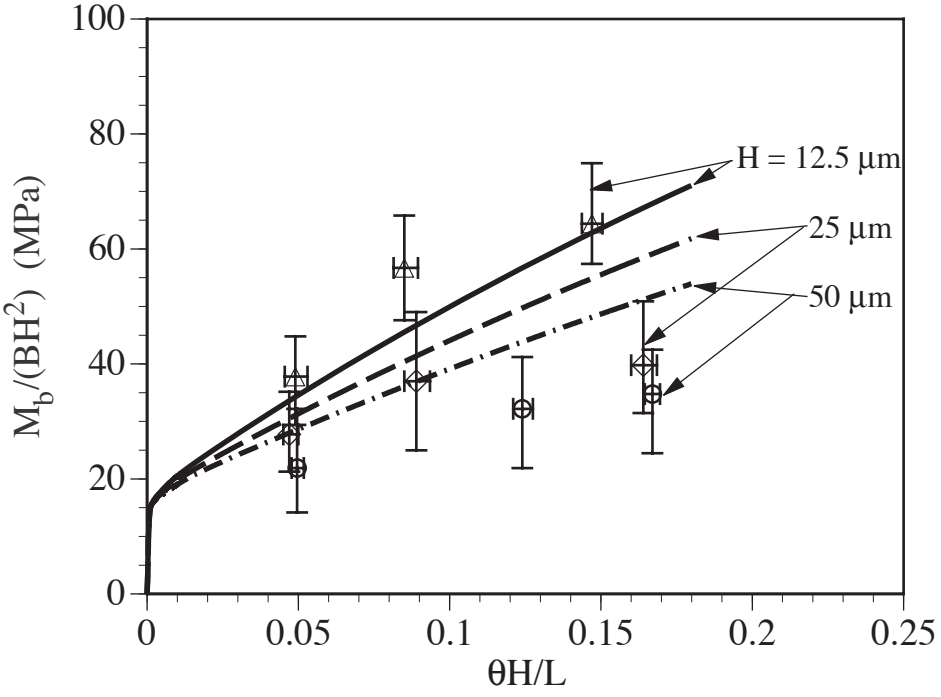

Figure 3. Comparison of computed curves of bending moment versus bending angle to experimental results of Stölken and Evans (1998).

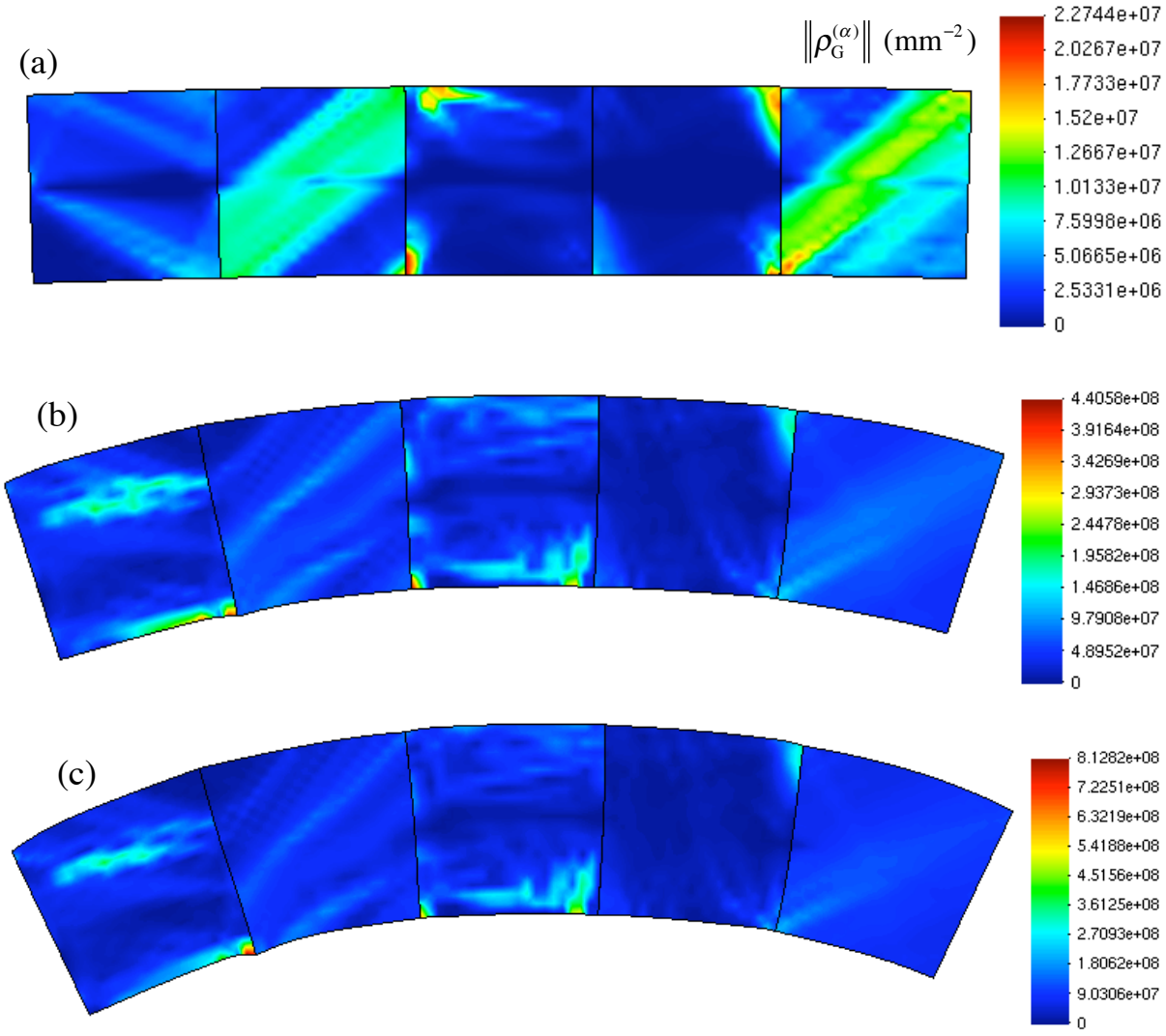

Figure 4. Deformed configurations of the foil ($H = 12.5\ \mu$m) and contours of GND densities on primary slip system at (a) $\theta H / L = 0.013$, (b) $\theta H / L = 0.123$, and (c) $\theta H / L = 0.178$.

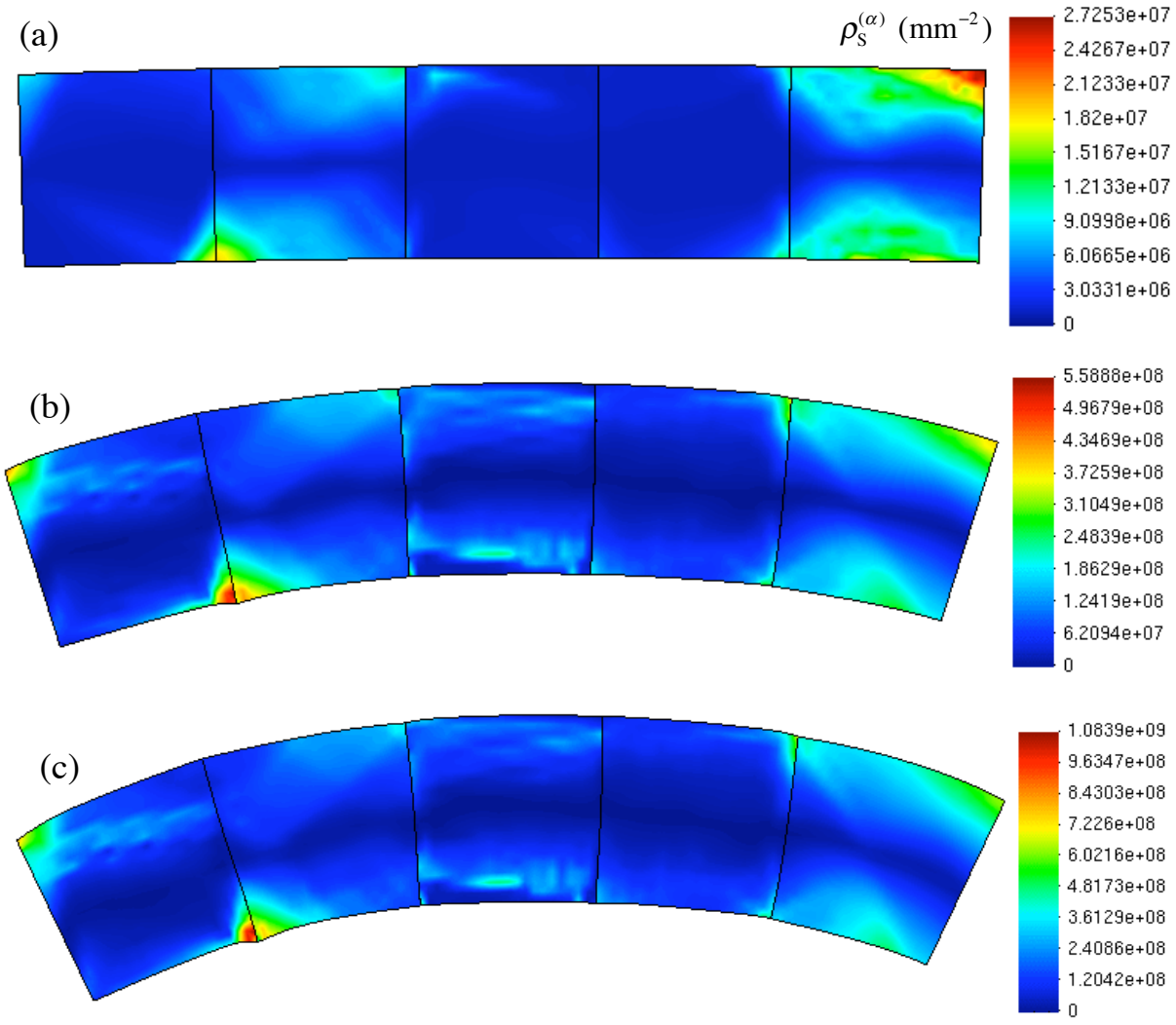

Figure 5. Deformed configurations of the foil ($H = 12.5\ \mu$m) and contours of SSD densities on primary slip system at (a) $\theta H / L = 0.013$, (b) $\theta H / L = 0.123$, and (c) $\theta H / L = 0.178$.